Platoon Control of Connected Multi-Vehicle Systems Under V2X Communications: Design and Experiments

Yongfu Li, *Member, IEEE*, Wenbo Chen, Srinivas Peeta, and Yibing Wang, *Member, IEEE*

***Abstract*— This paper focuses on platoon control of multi-vehicle systems in a realistic vehicle-to-vehicle/vehicle-to-infrastructure (V2V/V2I, or V2X) communication environment. To this end, the communication probability of the beacon transmission is analyzed based on the carrier sense multiple access with collision avoidance (CSMA/CA) mechanism. Then, a new car-following model is proposed by considering the communication probability to capture the car-following behavior of connected vehicles (CVs) equipped with V2X communications. The stability of the proposed car-following model is analyzed using the perturbation method. In addition, a nonlinear consensus-based longitudinal control algorithm is designed by considering the interactions between CVs, and an artificial function-based lateral control algorithm is presented. The convergence of the longitudinal and lateral control algorithms is analyzed using the Hurwitz stable theorem and Lyapunov technique, respectively. Also, the string stability of the vehicular platoon is performed based on the infinity-norm method. Finally, field experiments are conducted using four CVs under the scenarios of platoon forming, vehicle merging, and vehicle diverging. The results verify the effectiveness of the proposed method in terms of the trajectory and velocity profiles.**

***Index Terms*— Connected vehicle, platoon control, beacon transmission, car-following model, stability and consensus.**

I. Introduction

PLATOON-BASED driving patterns have the potential to mitigate traffic congestion, increase road throughput, and reduce energy consumption. Platoon efficiency can be enhanced by the emerging vehicle-to-vehicle and vehicle-to-infrastructure (V2V and V2I, or V2X) communications [1]–[7]. Platooning is referred to vehicles traveling together with a harmonized velocity and a small inter-vehicle gap, in which the close distance between vehicles leads to a decreased aerodynamic drag and an increase road capacity [8]–[9]. Consequently, many studies have been proposed in recent years related to platoon control [10]–[16]. The main idea of these studies from the control theory perspective is to treat each vehicle in the platoon as an individual agent and then design control algorithms involving the inter-vehicle gap and velocity to reach a consensus state. Many studies have addressed single lane discipline-based control algorithms that focus on the longitudinal dynamics. However, these control-focused studies have one or more of the following limitations: (i) they do not focus adequately on car-following interactions between vehicles, (ii) they do not consider the maneuvers of merging and diverging, (iii) the algorithms are verified primarily using simulation rather than real-world data, and (iv) their V2X connectivity assumptions can be idealized. However, from a real-world perspective, not only should the consensus of vehicles be ensured, but also the behavior of vehicles should be consistent with traffic flow principles. Hence, there is the key need to study platoon control with a focus on the interactions between vehicles. Further, there is the critical need for field data that can reflect realistic V2X communications.

This study is motivated by the need for a practical control strategy under the connected environment to fill the aforementioned gaps related to platoon control. In recent years, several studies investigated the effects of control strategy and communication topology on platoon control. In the control strategy context, Ghasemi *et al*. [17] proposed a double layer control framework, including a feedback linear controller and a proportional derivative controller, to analyze platoon control. Guo *et al*. [18] proposed a distributed adaptive integrated-sliding-mode controller for vehicle platoons. Dunbar and Caveney [19] proposed a distributed receding horizon control for vehicle platoons, with emphasis on stability and string stability. Bernardo *et al*. [20] presented a distributed control protocol considering time-varying heterogeneous delays. Recently, Li *et al*. [21] proposed a robust acceleration tracking control. Yu and Liu [22] designed a distributed controller for each follower, and the leader-follower formation is achieved

Manuscript received June 21, 2018; revised October 31, 2018 and January 2, 2019; accepted March 11, 2019. Date of publication April 11, 2019; date of current version May 1, 2020. This work was supported in part by the National Natural Science Foundation of China under Grant 61773082 and Grant 71771200, in part by the Foundation of Chongqing under Grant cstc2017jcyjBX0018, Grant cstc2018jszx-cyzdX0064, and Grant CX2017044, in part by the Foundation of Chongqing University of Posts and Telecommunications under Grant A2018-02, and in part by the National Key Research and Development Program under Grant 2016YFB0100906 and Grant 2018YFB1600502. The Associate Editor for this paper was L. Yang. *(Corresponding author: Yongfu Li.)*

Y. Li and W. Chen are with the Key Laboratory of Intelligent Air-Ground Cooperative Control for Universities in Chongqing, Chongqing University of Posts and Telecommunications, Chongqing 400065, China, and also with the Key Laboratory of Industrial IoT and Networked Control, Ministry of Education, College of Automation, Chongqing University of Posts and Telecommunications, Chongqing 400065, China (e-mail: liyongfu@cqupt.edu.cn).

S. Peeta is with the School of Civil and Environmental Engineering, Georgia Institute of Technology, Atlanta, GA 30332 USA, and also with the School of Industrial and Systems Engineering, Georgia Institute of Technology, Atlanta, GA 30332 USA (e-mail: srinivas.peeta@ce.gatech.edu).

Y. Wang is with the College of Civil Engineering and Architecture, Zhejiang University, Hangzhou 310058, China (e-mail: wangyibing@zju.edu.cn).

Digital Object Identifier 10.1109/TITS.2019.2905039

while satisfying velocity constraints. Defoort *et al*. [23] developed a coordinated control based leader-follower approach to achieve formation maneuvers. However, these control strategies focus on the longitudinal control of vehicle platoons, but less so on lateral control. Accordingly, they do not investigate the effects of the maneuvers of merging and diverging on platoon control.

In the context of consensus-based control, Su *et al*. [24] proposed an output feedback consensus algorithm. Qin *et al*. [25] analyzed the leader-following consensus in various settings. You and Xie [26] provided the necessary and sufficient conditions for the consensus of a multi-agent system. Zhang *et al*. [27] investigated the discrete-time optimal consensus control problem for multiple vehicles. Zhang *et al*. [28] proposed two observer-based event-triggered control protocols. These studies focused on single lane discipline-based consensus with respect to the vehicle position and velocity in the platoon. Li *et al*. [29], [30] proposed nonlinear finite-time consensus-based control strategies and consensus-based cooperative control for connected vehicles (CVs). However, they ignore the car-following interactions between vehicles, which should be ensured for consistency with traffic flow principles.

From the perspective of communication topology, under the V2X communications context, Seiler *et al*. [31] proposed a control strategy considering the spacing information with respect to both its immediate predecessor and follower. Zheng *et al*. [32] analyzed the stability and conducted simulations for some commonly-used communication topologies (e. g., two-predecessors following topology). Jia and Ngoduy [33] proposed a V2X communications topology for a cooperative driving system. Zheng *et al*. [34] analyzed the stability for a platoon connected through undirected information flow. However, these studies not only require communication links between the lead vehicle and following vehicle but also each pair of vehicles in the platoon, which increases the communication burden and deteriorate communication efficiency. In addition, these studies verify the performance using simulation only. They do not provide field experiments under realistic V2X communications to validate the analysis.

Motivated by the need for realistic V2X communications, this study seeks to design and implement connected multi-vehicle platoon control so as to ensure consensus while capturing the characteristics of CVs in the platoon. The contributions of this study are as follows:

(i) Related to car-following behavior of CVs under V2V communications, a new car-following model is proposed by considering the communication probability of the beacon transmission. The stability of the proposed car-following model is analyzed using the perturbation method.

(ii) Differing from the linear consensus-based control algorithms in [24]–[28] and [30] which only analyze longitudinal consensus and ignore the car-following behaviors between vehicles, this study proposes a nonlinear consensus-based longitudinal control algorithm that factors the car-following interactions between CVs. In addition, an artificial function-based lateral control algorithm is also designed.

(iii) The string stability of the platoon is performed based on the infinity-norm method. It can guarantee the attenuation of spacing error when moving away from the platoon leader.

(iv) In the performance evaluation context, field experiments are conducted for the scenarios of platoon forming, vehicle merging, and vehicle diverging using four CVs equipped with V2X devices (i.e., on-board unit/roadside unit (OBU/RSU)).

TABLE I
DEFINITIONS OF SOME COMMON SYMBOLS

Parameter	Definition
p_j	Probability of a successful beacon delivery of vehicle j.
$a_j(t)$	Longitudinal acceleration of vehicle j at time t.
$x_j(t)$	Longitudinal position of vehicle j at time t.
$v_j(t)$	Longitudinal velocity of vehicle j at time t.
$\Delta x_{i,j}(t)$	Longitudinal gap difference between vehicle i and vehicle j at time t.
$\Delta v_{i,j}(t)$	Longitudinal velocity difference between vehicle i and vehicle j at time t.

The remainder of this paper is organized as follows: Section II investigates the car-following behavior. Section III presents the platoon control strategy. Section IV discusses the field experiments conducted and their results. Concluding remarks are provided in Section V.

II. MODELING THE CAR-FOLLOWING BEHAVIOR

This section presents the communication topology, beacon transmission analysis, car-following model, and stability analysis of a connected multi-vehicle system under V2X communications. In addition, Table I summarizes notations for some widely-used symbols in this paper.

A. Communications Topology

This study considers a vehicle string consisting of N vehicles traveling on a straight road that includes a leader (labeled vehicle 0) and N-1 followers (labeled vehicles 1 to N-1). To balance communication efficiency and resource burden, we use the bidirectional-leader following (BDLF) communication topology to characterize the connectivity between vehicles under the V2X context. That is, every follower in the string has access to the real-time information (i.e., position and velocity) of only the leader. Further, the leader can obtain information from each follower through V2V communications. In addition, the follower has access to the local information of its immediate predecessor via a sensor (e.g., visual sensor). Fig. 1 shows the details of the BDLF communication topology. It is important to note here that in this study the RSU focuses on the selection of the leader, but does not affect the behavior of vehicles.

To specify the BDLF topology, a weighted directed graph $G = (V, E, B)$ is used in this study, where $V = \{0, 1, \cdots, N-1\}$ is the set of nodes, $E \subseteq V \times V$ is the set of edges, and B is a weighted adjacency matrix with nonnegative

TABLE II
ADJACENCY MATRICES FOR TOPOLOGIES RELATED TO THREE SCENARIOS

NO.	Adjacency matrix	NO.	Adjacency matrix	NO.	Adjacency matrix
(a)	$\begin{bmatrix} 0 & 0 & 0 & 0 & \cdots & 0 \\ 1 & \ddots & 0 & \cdots & \cdots & 0 \\ 1 & 0 & \ddots & \cdots & \cdots & \vdots \\ 1 & \vdots & \vdots & \ddots & \cdots & \vdots \\ \vdots & \vdots & \vdots & \vdots & \ddots & \vdots \\ 1 & 0 & \cdots & \cdots & \cdots & 0 \end{bmatrix}$	(b)	$\begin{bmatrix} 0 & 1 & 1 & 1 & \cdots & 1 \\ 0 & \ddots & 0 & \cdots & \cdots & 0 \\ 0 & 0 & \ddots & \cdots & \cdots & \vdots \\ 0 & \vdots & \vdots & \ddots & \cdots & \vdots \\ \vdots & \vdots & \vdots & \vdots & \ddots & \vdots \\ 0 & 0 & \cdots & \cdots & \cdots & 0 \end{bmatrix}$	(c)	$\begin{bmatrix} 0 & 0 & 1 & 1 & \cdots & 1 \\ 0 & \ddots & 0 & \cdots & \cdots & 0 \\ 2 & 0 & \ddots & \cdots & \cdots & \vdots \\ 1 & \vdots & \vdots & \ddots & \cdots & \vdots \\ \vdots & \vdots & \vdots & \vdots & \ddots & \vdots \\ 1 & 0 & \cdots & \cdots & \cdots & 0 \end{bmatrix}$
(d)	$\begin{bmatrix} 0 & 1 & 1 & 1 & \cdots & 1 \\ 1 & \ddots & 0 & \cdots & \cdots & 0 \\ 1 & 0 & \ddots & \cdots & \cdots & \vdots \\ 1 & \vdots & \vdots & \ddots & \cdots & \vdots \\ \vdots & \vdots & \vdots & \vdots & \ddots & \vdots \\ 1 & 0 & \cdots & \cdots & \cdots & 0 \end{bmatrix}$	(e)	$\begin{bmatrix} 0 & 0 & 1 & 1 & \cdots & 1 \\ 1 & \ddots & 0 & \cdots & \cdots & 0 \\ 1 & 0 & \ddots & \cdots & \cdots & \vdots \\ 1 & \vdots & \vdots & \ddots & \cdots & \vdots \\ \vdots & \vdots & \vdots & \vdots & \ddots & \vdots \\ 1 & 0 & \cdots & \cdots & \cdots & 0 \end{bmatrix}$	(f)	$\begin{bmatrix} 0 & 1 & 1 & 1 & \cdots & 1 \\ 2 & \ddots & 0 & \cdots & \cdots & 0 \\ 1 & 0 & \ddots & \cdots & \cdots & \vdots \\ 1 & \vdots & \vdots & \ddots & \cdots & \vdots \\ \vdots & \vdots & \vdots & \vdots & \ddots & \vdots \\ 1 & 0 & \cdots & \cdots & \cdots & 0 \end{bmatrix}$

elements. Here, $b_{ij} = 1$ if vehicle i has access to the information of vehicle j via sensor and/or V2V communications; otherwise $b_{ij} = 0$. For example, according to Fig. 1-a-(3) (right) as vehicle 1 can obtain information from vehicle 0 via sensor and/or V2V communications, the corresponding value in matrix (f) of Table II is $b_{10} = 2$. In addition, we assume there are no self-loops in the digraph, i.e., $b_{ii} = 0$.

Define $B = C + D$, where matrices $C = [c_{ij}]_{N\times N}$ and $D = [d_{ij}]_{N\times N}$ are adjacency matrices with nonnegative elements as well. $c_{ij} > 0$ and $d_{ij} > 0$ imply that vehicle i can obtain the information of vehicle j via sensor (e. g., visual sensor) and V2V communications, respectively; otherwise, $c_{ij} = 0$ and $d_{ij} = 0$. Matrix Γ is defined as $\Gamma = \text{diag}(\gamma_0, \gamma_1, \cdots, \gamma_{n-1})$, where $\gamma_i = d_{ij} \wedge d_{ji},\ j = 0$.

B. Beacon Transmission Analysis

Under the V2X context, the beacon is used to periodically disseminate vehicular information such as position, velocity, and direction. In this study, the CSMA/CA mechanism is used to analyze the beacon transmission performance [35].

According to the CSMA/CA mechanism, only one beacon is transmitted in the channel. Three cases are considered: for the channel (1) it is idle and no is beacon transmitted, (2) only one beacon is transmitted with success, and (3) more than one vehicle tries to send beacons in the channel, causing collisions. To facilitate beacon analysis, σ is defined as the slot time, $T_s = (T_h + L/R + T_{AIFS})/\sigma$ is the time duration of a successful transmission measured in slot time, where T_h is the duration of the physical layer convergence protocol preamble and header, L is the beacon length, R is the data rate, and T_{AIFS} is a time interval between frames being transmitted. $T_c = (T_h + L/R + T_{EIFS})/\sigma$ is the time duration of data collision, where T_{EIFS} is the cost time when the physical layer indicates a beacon is unsuccessfully transmitted. In addition, $T = (T_{CCH} - T_g - T_h - L/R)/\sigma - T_w$ is the useful duration, where T_{CCH} and T_g are the durations of the control channel (CCH) interval and the guard time, respectively. T_w is the back off time randomly selected from the contention window W. Initially, a beacon should wait with a random delay T_w, and is transmitted in the lth slot at time t. Accordingly, $p(T_t = t) = 1/W$ is defined as the probability of the transmission start time. The probability $p(l, N, W, k)$ implies that N vehicles in the communication network select back off time in W, but only k vehicles transmit in the lth slot. Hence, we have

$$\begin{aligned} &p(l, N, W, k) \\ &\quad = \left[1 - \sum_{t=0}^{l-1} p(T_t = t)\right]^N \binom{N}{k} \times \left[\frac{p(T_t = l)}{1 - \sum_{t=0}^{l-1} p(T_t = t)}\right]^k \\ &\qquad \times \left[1 - \frac{p(T_t = l)}{1 - \sum_{t=0}^{l-1} p(T_t = t)}\right]^{M-k}, \end{aligned} \tag{1}$$

where $\sum_{t=0}^{l-1} p(T_t = t)$ denotes the probability that $(l - 1)$ slots pass before the first transmission attempt, and $p(T_t = l)/1 - \sum_{t=0}^{l-1} p(T_t = t)$ denotes the probability of choosing any slot in the remaining $(T + W - 1)$ slots.

Based on (1), $X(t, N)$ is further defined as the mean number of N vehicles that successfully transmit beacons during each CCH interval. Note that t is the slots left in this interval and $X(t, N)$ can be calculated as follows:

$$\begin{aligned} X(t, N) = \sum_{l=0}^{t} \{&p(l, N, W, 1)[1 + X(t - l + 1 - T_s, N - 1] \\ &+ \sum_{k=2}^{M} p(l, N, W, k) X\,(t - l + 1 - T_c, N - k)\}, \end{aligned} \tag{2}$$

where the first two terms in (2) denote the probability that one of N vehicles transmits in the lth slot with the choice of back off from W slots. $X\,(t - l + 1 - T_s, N - 1)$ is the mean number of successful transmissions in the remaining $t - l + 1 - T_s$ slots. The third term denotes that k of N vehicles transmit in the lth slot and thus cause collisions [35].

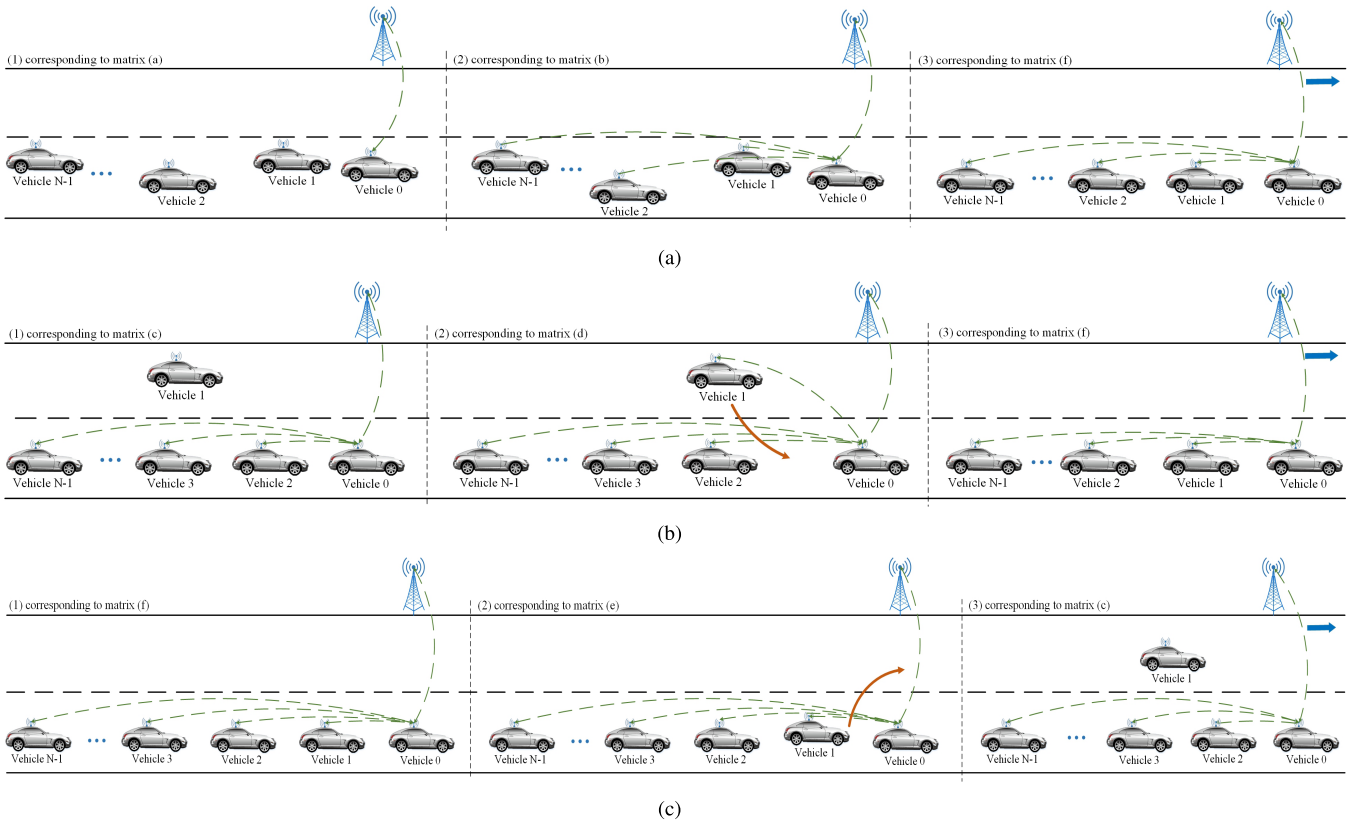

Fig. 1. Communication topologies of three scenarios. (a) Platoon forming. (b) Vehicle merging. (c) Vehicle diverging.

As a result, the probability of a successful beacon delivery of vehicle j under the BDLF topology can be calculated as

$$p_j = \frac{X(t, N-1)}{N-1}, \tag{3}$$

Note that $p_j = 1$ if $p_j \geq \omega$; otherwise, $p_j = 0$. $\omega = 0.6$ is the threshold value.

Remark 1: The selection of the threshold value seeks to illustrate that vehicular information can be successfully exchanged in the CV context when the probability is large enough. In this study, we set $\omega = 0.6$ to ensure that reliable information exchange can occur between vehicles if $p_j \geq \omega$. For example, if $p_j = 0.1$, the probability of successful beacon delivery is too small to guarantee information exchange.

Remark 2: According to [35], the maximum waiting time, T_{wait}, of the beacon transmission is $T_{wait} = (N-1) \cdot T_s + [W - (N-1) - 1]$ when $2 < N \leq W$, where N is vehicle number, and W is contention window size. In the following experiments performed in Sec. IV, we choose $W = 8$ and $N = 4$. Hence, $T_{wait} = 26.81$ slots. It is about 4.29×10^{-4}s if the slot time is 16μs. In addition, the average end-to-end communication delay in IEEE 802.11p is of the order of hundredths of a second (i.e., 10^{-2}s) [36]. Based on the time taken in a practical application, this study does not take T_{wait} and the communication delay into consideration.

C. Car-Following Behavior

To capture the car-following behavior of CVs in the same lane without lane-change, a new car-following model can be formulated as follows:

$$\begin{aligned} a_j(t) = m\{&V(\Delta x_{j,j-1}(t)) + p_j\alpha_j[V(\Delta x_{j,0}(t)) \\ &- V(\Delta x_{j,j-1}(t))] - v_j(t)\} \\ &+ \lambda[(1 - p_j\alpha_j)\Delta v_{j,j-1}(t) + p_j\alpha_j \Delta v_{j,0}(t)], \end{aligned} \tag{4}$$

where $k > 0$ and $\lambda \geq 0$ are constant sensitivity coefficients. $\alpha_j = 1/j^{j-1}$ is the weight factor. $V(\cdot)$ is the optimal velocity of a vehicle which is determined by the longitudinal inter-vehicle gap between the following vehicle and its immediate predecessor [5]. It is defined as:

$$V(\Delta x) = V_1 + V_2 \tanh(J_1(\Delta x - L_v) - J_2), \tag{5}$$

where V_1, V_2, J_1, J_2 are positive constants, and L_v is the vehicle length.

Remark 3: Compared to [5], [37], and references therein, the proposed car-following model incorporates the communication probability of the beacon transmission, which is more realistic in the V2X communications context.

D. Stability Analysis

The stability of the proposed car-following model is analyzed using the small perturbation method, starting from the following assumption:

Assumption 1: The traffic flow is initially in equilibrium which is characterized by an identical equilibrium gap h associated with the identical equilibrium velocity $V(h)$.

Theorem 1: The uniform traffic flow in (4) is stable if

$$\dot{V}(h) < \frac{m(1-p_j\alpha_j+p_j\alpha_j j^2)}{2(1-p_j\alpha_j+p_j\alpha_j j)^2}+\lambda, \tag{6}$$

where $\dot{V}(h)=\frac{\partial V(\Delta x)}{\partial \Delta x}\Big|_{\Delta x=h}$.

Proof: Following Assumption 1, the position solution is:

$$x_j^0(t)=(N-j)h+V(h)t, \tag{7}$$

where $x_j^0(t)$ is the position of vehicle j in steady state.

Adding a small disturbance $y_j(t)$ to $x_j^0(t)$ yields:

$$x_j(t)=x_j^0(t)+y_j(t). \tag{8}$$

Substituting (8) into (4), and linearizing the resulting equation using Taylors expansion yields:

$$\begin{aligned}\ddot{y}_j(t)=&\, m\{\dot{V}(h)\Delta y_{j,j-1}(t)+p_j\alpha_j\dot{V}(h)\\ &\times(\Delta y_{j,0}(t)-\Delta y_{j,j-1}(t))]-\dot{y}_j(t)\}\\ &+\lambda[(1-p_j\alpha_j)\Delta\dot{y}_{j,j-1}(t)+p_j\alpha_j\Delta\dot{y}_{j,0}(t)].\end{aligned} \tag{9}$$

Rewriting $y_j(t)$ in the Fourier mode and substituting it into (9) yields:

$$\begin{aligned}z^2=&\, m\{\dot{V}(h)[(1-p_j\alpha_j)(e^{\mathrm{i}\beta}-1)+p_j\alpha_j(e^{\mathrm{i}\beta j}-1)]-z\}\\ &+\lambda[(1-p_j\alpha_j)z(e^{\mathrm{i}\beta}-1)+p_j\alpha_j z(e^{\mathrm{i}\beta j}-1)].\end{aligned} \tag{10}$$

Let $z=z_1(\mathrm{i}\beta)+z_2(\mathrm{i}\beta)^2+\cdots$ using the long wave method, and expanding it to the second term of $(\mathrm{i}\beta)$. Thus, we have

$$\begin{cases} z_1=\dot{V}(h)(1-p_j\alpha_j+p_j\alpha_j j)\\ z_2=\frac{1}{2}\dot{V}(h)[1-p_j\alpha_j+p_j\alpha_j j^2]\\ \quad+\dfrac{[\lambda\dot{V}(h)+\dot{V}^2(h)][(1-p_j\alpha_j)+p_j\alpha_j j]^2}{k}, \end{cases} \tag{11}$$

when $z_1>0$ and $z_2>0$, the stability condition shown in (6) can be derived. The proof is complete. □

Simulation experiments are performed to verify the stability of the proposed car-following model. In Fig. 2, the value of λ is set as 0.1, and p_j is set as 1.0, 0.8 and 0.6. The space is divided into two regions by the critical curve. The region above each critical curve is the stable region where traffic flow is stable, while the region below is the unstable region where density waves emerge.

Remark 4: The stability analysis further illustrates that the steady-state performance of the proposed model is improved in terms of the stability region [37], [38]. In addition, when $p_j=0$, the stability region of the proposed model is the same as that of the model in [38]. It implies that the proposed model is more generalized than the model in [38].

III. Platoon Control Design

This section presents longitudinal and lateral platoon control algorithms, convergence analysis, and string stability analysis. The longitudinal and lateral control algorithms are used to compute the advisory velocity of vehicle in the field experiments.

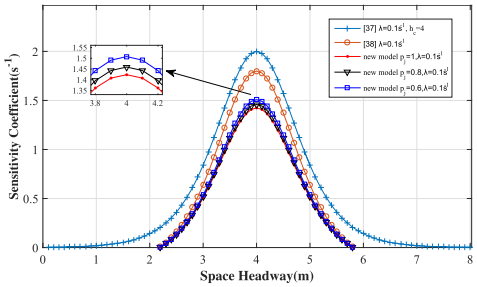

Fig. 2. Critical curves between sensitivity coefficient and space headway.

A. Longitudinal Controller

The consensus-based controller is designed as follows:

$$\begin{cases} \dot{x}_i(t)=v_i(t)\\ \dot{v}_i(t)=-\sum\limits_{j=0}^{n-1}C_{ij}[\delta(V(h_{i,j}(t))-v_i(t))\\ \quad+(x_i(t)-x_j(t)-r_{i,j})+\mu(v_i(t)-v_j(t))]\\ \quad-\gamma_i[(x_i(t)-x_0(t)-r_i)+\rho(v_i(t)-v_0(t))], \end{cases} \tag{12}$$

where $h_{i,j}=\frac{x_i(t)-x_j(t)}{j-i}$ is the average longitudinal gap between vehicle i and j, and r_i the desired longitudinal gap between vehicle i and the leader. $r_{i,j}$ is the desired longitudinal gap between vehicle i and j. δ, μ and ρ are the gain parameters. Under the BDLF topology shown in Fig. 1, the follower has access to the information of the leader; hence, $d_{i0}=1$.

Remark 5: The linear controllers in [24]–[27] and [31]–[34] ignore the interactions between vehicles, resulting in negative velocity and negative spacing error, which is unreasonable in practice. By contrast, the proposed nonlinear controller (12) incorporates the car-following interactions between vehicles (i.e., $V(\cdot)$). Thereby, vehicles can smoothly reach the consensus state with respect to position and velocity, and the behavior of vehicles is consistent with traffic flow theory.

B. Lateral Controller

To design the lateral controller, following the approach used in [39], an artificial function is designed as:

$$g(y)=(y-L_r)/L_r y,\quad 0<y\le 2L_r, \tag{13}$$

where y is the distance of vehicle to the right boundary, and L_r is half the lane width. Based on (13), the lateral controller is designed as [39]:

$$\begin{aligned}g_i=&-G_1\sum_{\kappa=1}^{2}g(\|\bar{y}_{i,L_\kappa}-y_i\|_\sigma)n_{i,L_\kappa}\\ &+G_2\sum_{\kappa=1}^{2}(\bar{\psi}_{i,L_\kappa}-\psi_i),\end{aligned} \tag{14}$$

where ψ_i is the lateral velocity of vehicle i, L_κ is the boundary of lane $\kappa=1,2$, $\bar{y}_{i,L_\kappa}$ and $\bar{\psi}_{i,L_\kappa}$ are the position and velocity projections of vehicle i on the lateral boundary L_κ,

respectively, $G_1 > 0$ and $G_2 > 0$ are constant parameters, and g_i is the lateral acceleration. The σ-norm $||\cdot||_\sigma$ is defined by:

$$||z||_\sigma = (\sqrt{1 + q||z||^2} - 1)/q, \tag{15}$$

where the parameter $q > 0$. In addition, the coefficient n_{i,L_k} is defined as

$$n_{i,L_\kappa} = \frac{\bar{y}_{i,L_\kappa} - y_i}{\sqrt{1 + \zeta \left\| \bar{y}_{i,L_\kappa} - y_i \right\|_\sigma^2}}, \tag{16}$$

where $\zeta > 0$ is a constant.

C. Longitudinal Convergence Analysis

To facilitate the convergence analysis based on (12), we first define $\tilde{x}_i(t) = x_i(t) - x_0(t) - r_i$. Thereby, we have:

$$\begin{cases} \dot{\tilde{x}}_i(t) = \tilde{v}_i(t) \\ \dot{\tilde{v}}_i(t) = -\sum\limits_{j=0}^{n-1} C_{ij}[\delta(V(h_{i,j}(t)) \\ \quad - V(h^*_{i,j}(t)) - \tilde{v}_i(t)) + (\tilde{x}_i(t) - \tilde{x}_j(t)) \\ \quad + \mu(\tilde{v}_i(t) - \tilde{v}_j(t))] - \gamma_i[\tilde{x}_i(t) + \rho\tilde{v}_i(t)] \end{cases} \tag{17}$$

Note that $V(h_{i,j}(t)) - V(h^*_{i,j}(t)) = \frac{\dot{V}(h^*_{i,j}(t))}{j-i}(\tilde{x}_i(t) - \tilde{x}_j(t))$ and $\varphi_{i,j}(\xi_{i,j}(t)) = \frac{\dot{V}(h^*_{i,j}(t))}{j-i}$. It follows from (17) that:

$$\begin{cases} \dot{\tilde{x}}_i(t) = \tilde{v}_i(t) \\ \dot{\tilde{v}}_i(t) = -\sum\limits_{j=0}^{n-1} C_{ij}[\delta(\varphi_{i,j}(\xi_{i,j}(t) + 1)(\tilde{x}_i(t) - \tilde{x}_j(t) \\ \quad + (\mu - \delta)\tilde{v}_i(t) - \mu\tilde{v}_j(t))] - \gamma_i[\tilde{x}_i(t) + \rho\tilde{v}_i(t)] \end{cases} \tag{18}$$

Let $\tilde{\boldsymbol{x}} = [\tilde{x}_1, \cdots, \tilde{x}_n]^{\mathrm{T}}$, $\tilde{\boldsymbol{v}} = [\tilde{v}_1, \cdots, \tilde{v}_n]^{\mathrm{T}}$, $\tilde{\boldsymbol{\varepsilon}} = [\tilde{x}^{\mathrm{T}}\tilde{v}^{\mathrm{T}}]^{\mathrm{T}}$. (18) can be rewritten as:

$$\dot{\tilde{\boldsymbol{\varepsilon}}}(t) = A\tilde{\boldsymbol{\varepsilon}}(t), \tag{19}$$

where $A = \begin{bmatrix} 0_{n\times n} & \mathrm{I}_{n\times n} \\ (\delta\varphi_{i,j}+1)(O-C_j)-\Gamma_i & (\mu-\delta)O-\mu C_j-\Gamma_i\rho \end{bmatrix}$, $C_j = \begin{bmatrix} 0 \cdots c_{1j} \cdots 0 \\ 0 \cdots c_{2j} \cdots 0 \\ \vdots \cdots \vdots \cdots \vdots \\ 0 \cdots c_{nj} \cdots 0 \end{bmatrix}$, and $O = \mathrm{diag}(o_1, \cdots, o_n)$, $o_i = \sum_{j=1}^{n} c_{ij}$.

Lemma 1 [40]: Given a complex-coefficient polynomial

$$r(z) = z^2 + (a + ib)z + c + id, \tag{20}$$

where $a, b, c, d \in \mathrm{R}$, $r(z)$ is Hurwitz stable if and only if $a > 0$ and $abd + a^2c - d^2 > 0$.

Theorem 2: Under the controller (12), if $\delta > 0$, $\mu > 0$ and $\rho > 0$, we have

$$\lim_{t\to\infty} \tilde{\varepsilon}(t) = 0. \tag{21}$$

Proof: Let λ be the eigenvalue of A, then

$$\begin{aligned} \det(\lambda I_{2n} - A) &= \begin{vmatrix} \lambda I_{n\times n} & -I_{n\times n} \\ -(\delta\varphi_{i,j} + 1) & \lambda I_{n\times n} - (\mu - \delta) \\ \times(O - C_j) + \Gamma_i & \times O + \mu C_j + \Gamma_i\rho \end{vmatrix} \\ &= \det(\lambda^2 I_{n\times n} + H_1\lambda I_{n\times n} + H_2), \end{aligned} \tag{22}$$

where $H_1 = \mu C_j - (\mu - \delta)O + \Gamma_i\rho$ and $H_2 = -(\delta\varphi_{i,j} + 1)(O - C_j) + \Gamma_i$.

To guarantee matrix A is Hurwitz stable, let $\theta_i \in \sigma(H_1)$, $\zeta_i \in \sigma(H_2)$, $i = 1, \cdots, n$. $\sigma(H_1)$ is the set of all eigenvalues of H_1 and $\sigma(H_2)$ is the set of all eigenvalues of H_2. Then, (22) can be rewritten as:

$$\det(\lambda I_{2n} - A) = \prod_{i=1}^{n} \lambda^2 + \theta_i\lambda + \zeta_i. \tag{23}$$

Thus, the Hurwitz stability of matrix A is equivalent to that of polynomial: $R(\lambda) = \lambda^2 + \theta_i\lambda + \zeta_i$, for all $\theta_i \in \sigma(H_1)$, $\zeta_i \in \sigma(H_2)$. Based on Lemma 1 and $\delta > 0$, $\mu > 0$ and $\rho > 0$, we have:

(1) $\mathrm{Re}(\theta_i) > 0$, which holds by the positive definite matrix A.
(2) $\mathrm{Re}(\theta_i)\mathrm{Im}(\theta_i)\mathrm{Im}(\zeta_i) + \mathrm{Re}^2(\theta_i)\mathrm{Re}(\zeta_i) - \mathrm{Im}^2(\zeta_i) > 0$.

Consequently, we have that matrix A is Hurwitz stable according to statements (1) and (2). Then, (12) is asymptotically stable. It implies that $\tilde{\varepsilon}(t) \to 0$ as $t \to \infty$. This completes the proof. □

D. Lateral Convergence Analysis

Theorem 3: Consider N vehicles moving in a straight lane, and assume the initial total energy $E_0 = E(y(0), \psi(0))$ are known, and $||y_{i,L_\kappa}(t) - \bar{y}_i(t)|| \geq 1$ holds. Then, under controller (14), the platoon approaches stability, and the following holds:

(a) The distance between vehicle i and the corresponding boundary in the lateral direction satisfies:

$$1 \leq ||y_i - \bar{y}_{i,L_\kappa}||_\sigma \leq \min\{2L, e^{E_0/\Phi_1}\}, \tag{24}$$

where Φ_1 is a constant positive factor.

(b) Vehicles in a string can converge to the midline, i.e.,

$$\lim_{t\to\infty} ||y_i(t) - \bar{y}_{i,L_\kappa}(t)|| = L_r. \tag{25}$$

(c) The velocity error of each vehicle i will converge to zero, i,e.,

$$\lim_{t\to\infty} ||\psi_i(t) - \bar{\psi}_{i,L_\kappa}(t)|| = 0. \tag{26}$$

The proof of Items (a)-(c) is similar to [39], and is omitted here.

E. String Stability of Vehicle Platoon

To facilitate string stability analysis, the following definition is provided.

Lemma 2 (Barbalat Lemma) [4]: If $\phi(t)$: $\mathrm{R} \to \mathrm{R}$ is a uniformly continuous function for $t \geq 0$ and $\lim_{t\to\infty} \int_0^t \phi(\tau)\mathrm{d}\tau < \infty$, then $\lim_{t\to\infty} \phi(t) = 0$.

Definition 1 (String Stability) [41]: Origin $x_i = 0$, with $i \in N$ and the dynamics in (17), is string stable if, given any $\Theta > 0$, there exists $\Xi > 0$ such that

$$\|e_i(0)\|_\infty < \Theta \Rightarrow \sup_i \|e_i(\cdot)\|_\infty < \Xi \tag{27}$$

TABLE III
IEEE 802.11P PARAMETERS [35], [42]

Parameter	Value	Parameter	Value
Channel width	10 MHz	Symbol duration	8 μs
Guard time	1.6 μs	EIFS	188 μs
Slot time	16 μs	AIFS	71 μs
Contention Window	8	Beacon frequency	10 Hz
Header duration	40 μs	CCHI	46 ms
Beacon size	64 bytes	Channel data rate	6 Mbps

Theorem 4: Considering the scenario shown in Fig. 1, the vehicle platoon is string stable under control algorithm (12) in the sense of Definition 1.

Proof: Define the longitudinal gap error as

$$e_i(t) = x_{i-1}(t) - x_i(t) - s \tag{28}$$

where s is the desired longitudinal gap in the stable platoon.

Given that $a_{i-1}(t)$ and $a_i(t)$ are bounded, and noting that $\ddot{e}_i(t) = a_{i-1}(t) - a_i(t)$, it implies that $\ddot{e}_i(t) \in \mathcal{L}_\infty$. Hence, $\dot{e}_i(t)$ is uniformly continuous.

In addition,

$$\int_0^\infty |\dot{e}_i(t)|\mathrm{d}t = |e_i(\infty)| - |e_i(0)| < \infty \tag{29}$$

According to (29), we know that $\dot{e}_i(t) \in \mathcal{L}_2$. Hence, we have $\lim_{t\to\infty} \dot{e}_i(t) = 0$ based on Lemma 2. Consequently, we know $\dot{e}_i(t) \in \mathcal{L}_\infty$. Similarly, since $e_i(0) = 0$, we have $e_i(t) \in \mathcal{L}_2$. Hence, we further have $\lim_{t\to\infty} e_i(t) = 0$ based on Lemma 2.

If $\xi > 0$, then $\|e_i(0)\|_\infty = \sup_i |e_i(0)| = 0 < \xi$. In addition, note that $\lim_{t\to\infty} e_i(t) = 0$, $e_i(0) = 0$, and $e_i(t) \in \mathcal{L}_2$. Hence, $\exists\ M, \eta > 0$, s.t. $\sup_{t\in[0,\infty)} |e_i(t)| = M < \eta$ for $t \in [0, \infty)$. Thereby, the string stability of the vehicle platoon with algorithm (12) can be guaranteed according to (27). The proof is completed. □

Remark 6: According to the string stability definition in [41], we analyzed the string stability based on the infinity-norm method. The results illustrate that the vehicle platoon can dissipate perturbation effects.

IV. EXPERIMENTS

This section discusses field experiments to validate the theoretical analyses.

A. Communication Devices

To perform the experiments, four equipped vehicles are used in the field experiments. The relevant devices including vehicles, OBUs, RSUs, and human machine interface (HMI), are shown in Fig. 3. Note that IEEE 802.11p is the protocol to facilitate communication links. The values of parameters associated with IEEE 802.11p are shown in Table III. The communication flows in the experiments are shown in Fig. 4.

The OBU consists of the differential global positioning system (DGPS), master chip, and DSRC module. The RSU includes the control box, DSRC module, and DGPS. The RSU can obtain information (e. g., traffic flow) by receiving state information from vehicles. The RSU can admit or reject

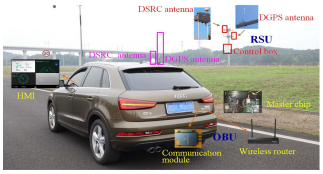

Fig. 3. Relevant devices.

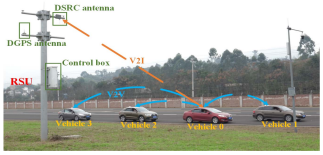

Fig. 4. Communication flows.

Fig. 5. Road condition.

the platoon forming request message (PFRM) according to traffic conditions. The HMI is used to display the real-time information and broadcast the advisory and lane-change information by voice.

In the experiments, a vehicle perceives the states of surrounding vehicles and infrastructure within the V2X communication range via DSRC. In addition, the master chip acquires the positioning information from the DGPS module, and sends the necessary real-time information (e.g., current velocity, advisory velocity, and lane-change information) to HMI via the Ethernet.

The HMI can broadcast the advisory velocity and lane-change information by voice. The advisory velocity of a vehicle is computed according to (12) and (14). The lane-change information is obtained based on the DGPS location.

Remark 7: In the field experiments, when the following vehicle moves in the same lane as its immediate predecessor, the driver will follow the advisory velocity displayed by the HMI and maintain a stable platoon formation. Otherwise, the following vehicle will take the maneuver of lane-change based on the HMI prompt so as to maintain the same lane as its immediate predecessor. Then, it adjusts its velocity according to the HMI to maintain a stable platoon formation.

B. Platoon Maneuvers

Three typical maneuvers, including platoon forming, vehicle merging, and vehicle diverging are analyzed in this study. Thereby, the communication topology between vehicles is analyzed in the following three scenarios. Table IV presents the variables used in this section. Fig. 5 is an aerial photo of the field experiment facility.

TABLE IV
DESCRIPTIONS OF VARIABLES IN THE PSEUDO-CODE

Variable	Unit	Description
ε_i	—	Lane number of vehicle i.
$v_{p_i}(t)$	km/h	Velocity of vehicle i at time t in experiments.
v_s	km/h	Stable velocity of the platoon.
$d_{i-1,i}(t)$	m	Longitudinal gap difference between vehicle i and vehicle i at time $t$at time t.
Δ	m	Additional gap between two CVs.

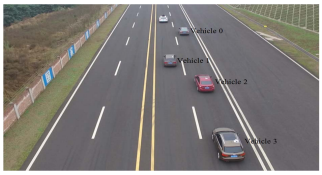

Fig. 6. Initially state of CVs.

Fig. 7. Merging maneuver.

Fig. 8. Diverging maneuver.

1) Platoon Forming: In this scenario, Fig. 1-a illustrates the maneuver of platoon forming, and it refers to the join-at-tail maneuver. During this process as shown in Fig. 1-a-(1) (left), vehicle 0 first sends a PFRM via the OBU to the RSU, and the RSU will return a platoon forming confirmation message (PFCM) to vehicle 0. The PFCM contains the information related to platoon ID, leader ID, and destination. Then, vehicle 0 becomes the leader of the platoon and it will periodically broadcast the platoon state message (PSTM), including platoon length, platoon ID, leader ID and destination, to other vehicles in the range of V2V communications.

When the surrounding vehicles receive the PSTM, as shown in Fig. 1-a-(2) (middle), they will send platoon merging request messages (PMRMs) to the leader. If the leader admits the merging request, it will return platoon control messages (PCTMs) to the joining vehicles. The PCTMs contain messages related to the advisory velocity and lane-changing.

Consequently, a joining vehicle can adjust its state to perform a join-at-tail maneuver followed by the PCTMs. If the platoon forming is completed as shown in Fig. 1-a (right), the joining vehicle will send the vehicle state messages (VSTMs), including vehicle ID, velocity, and location to the leader. In addition, the leader will broadcast the PCTMs to other members in the platoon so as to guarantee the platoon pattern.

TABLE V
PSEUDO-CODE OF PLATOON FORMING

	Initial state: N vehicles are moving in a lane
	Input: Dataset $\varepsilon_0 = \varepsilon_1 = \cdots = \varepsilon_{N-1} = 0$, $v_{p_0}(t) \neq v_{p_1}(t) \neq \cdots \neq v_{p_{N-1}}(t)$ $d_{0,1}(t) \neq d_{1,2}(t) \neq \cdots \neq d_{N-2,N-1}(t)$
1	Vehicle i sends PFRM to the nearby RSU
2	While True:
3	Case vehicle i:
4	if PFCM = True:
5	set $v_{p_i}(t) = v_s$
6	broadcast PSTM
7	if PMRM = True: return back PCTM
8	Default:
9	if PSTM = True: send PMRM to vehicle i
10	if PCTM = True:
11	for j in $0, \cdots, i-1, i+1, \cdots N-1$
12	if $d_{j-1,j}(t) > s$: increase $v_{p_j}(t)$
13	if $d_{j-1,j}(t) = s$: maintain $v_{p_j}(t) = v_s$
14	if $d_{j-1,j}(t) < s$: decrease $v_{p_j}(t)$
15	End
	Output: A platoon with N members are moving stably in a lane.

The platoon forming maneuver is performed using the adjacency matrices in Table I in the order a $\rightarrow$ b $\rightarrow$ f, which correspond to Fig. 1-a left-middle-right. The specific operations are shown in Table V.

In the experiment, initially, vehicles 0, 2 and 3 move in the same lane as shown in Fig. 6. Vehicle 0 is the leader, and vehicles 2 and 3 perform a join-at-tail maneuver. As a result, a three-vehicle platoon is formed. The longitudinal and lateral gaps between every vehicle pair of the platoon are $s = 25$m and 0m, respectively, and the desired stable velocity of the platoon is $v_s = 37$km/h.

2) Vehicle Merging: The maneuver of vehicle merging refers to a vehicle joining the platoon at the middle of the platoon. Fig. 1-b-(1) (left) illustrates a string of vehicles moving as a platoon in a lane on a road initially, and vehicle 1 moving in an adjacent lane. We assume that a vehicle (e. g. vehicle 1) is going to merge into the platoon. When vehicle 1 receives the PSTM via the OBU in the range of V2V communications, it will send a vehicle merging request message (VMRM), including the vehicle ID and current location, to the leader, as shown in Fig. 1-b-(2) (middle). After received the VMRM, the leader will determine the cut-in position of vehicle 1, and then send a deceleration command to vehicle 2 to N-1 in the platoon. Note that all commands sent from the leader are contained in the PCTM. As a result, the longitudinal gap between vehicle 0 and vehicle 2 will be widened. If the longitudinal gap is wide enough (i.e., $s + \Delta$), the leader will send a lane-change command to vehicle 1, and it will merge into the platoon. After vehicle 1 merges into the platoon, the leader will send commands to all members of the platoon to guarantee that it moves stably as in Fig. 1-b-(3) (right).

According to the vehicle merging maneuver, the switching communication links can be described using the adjacency matrices in Table I in the order c $\rightarrow$ d $\rightarrow$ f, which follows

TABLE VI

PSEUDO-CODE OF VEHICLE MERGING

	Initial state: A platoon with N-1 members is moving in a lane and vehicle i is moving in the adjacent lane
	Input: Dataset $\varepsilon_0 = \cdots = \varepsilon_{i-1} = \varepsilon_{i+1} = \cdots = \varepsilon_{N-1} = 0$, $\varepsilon_i = 1$, $v_{p_0}(t) = v_{p_1}(t) = \cdots = v_{p_{N-1}}(t) = v_s$, $d_{0,1}(t) = \cdots = d_{i-1,i+1}(t) = \cdots = d_{N-2,N-1}(t) = s$
1	Vehicle i sends VMRM to the platoon
2	While True:
3	Case leader:
4	if VMRM = True:
5	determine the inserting location $(i-1, i+1)$
6	return PCTM to vehicle i
7	send PCTM to vehicle i+1
8	Case vehicle i:
9	if PCTM = True:
10	if $d_{i-1,i+1}(t) = s + \Delta$:
11	lane-change operation, set $\varepsilon_i = 0$
12	Case vehicle i+1:
13	if PCTM = True:
14	if $d_{i-1,i+1}(t) > s + \Delta$: increase $v_{p_{i+1}}(t)$
15	if $d_{i-1,i+1}(t) = s + \Delta$: maintain $v_{p_{i+1}}(t)$
16	if $d_{i-1,i+1}(t) < s + \Delta$: decrease $v_{p_{i+1}}(t)$
17	End
	Output: A platoon with N members are moving stably in a lane.

TABLE VII

PSEUDO-CODE OF VEHICLE DIVERGING

	Initial state: A platoon with N members is moving in a lane
	Input: Dataset $\varepsilon_0 = \varepsilon_1 = \cdots = \varepsilon_{N-1} = 0$, $v_{p_0}(t) = v_{p_1}(t) = \cdots = v_{p_{N-1}}(t) = v_s$, $d_{0,1}(t) = d_{1,2}(t) = \cdots = d_{N-2,N-1}(t) = s$
1	Vehicle i sends VDRM to the platoon
2	While True:
3	Case leader:
4	if VMRM = True: return PCTM to vehicle i
5	if $\varepsilon_i = 1$: send PCTM to the platoon members
6	Case vehicle i:
7	if PCTM = True:
8	lane-change operation, set $\varepsilon_i = 1$
9	Default:
10	if PCTM = True:
11	maintain $d_{0,1}(t) = \cdots = d_{i-1,i+1}(t) = \cdots = d_{N-2,N-1}(t) = s$
12	End
	Output: A platoon with N-1 members are moving stably in a lane and vehicle i is moving in the adjacent lane.

Fig. 1-b left-middle-right. The vehicle merging procedures are listed in Table VI.

In the experiments, the platoon with vehicles 0, 2, and 3 moves stably in a lane, and vehicle 1 moves in an adjacent lane. Vehicle 1 is used to perform vehicle merging maneuver as shown as Fig. 7. The additional longitudinal gap when the vehicle is merging is set as $\Delta = 10$m. As a result, a platoon with four equipped vehicles is formed and moves stably.

3) Vehicle Diverging: Fig. 1-c-(1) (left) shows a string of vehicles moving as a platoon. When vehicle 1 sends a vehicle diverging request message (VDRM) to the leader as shown in Fig. 1-c-(2) (middle), the leader will return a PCTM to vehicle 1, and vehicle 1 will diverge from the platoon through a lane-change operation. Fig. 1-c-(3) (right) shows that the leader will send commands to other members in the platoon

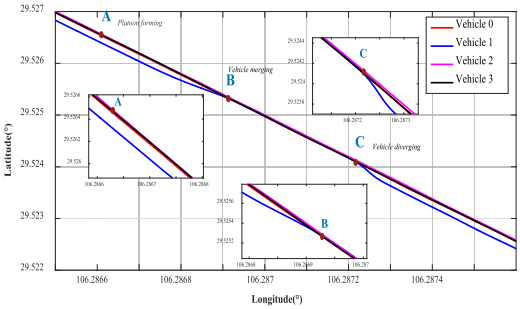

Fig. 9. Trajectories.

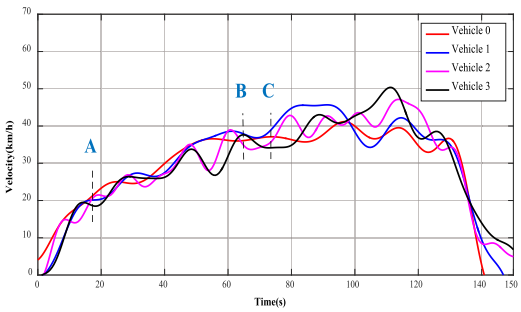

Fig. 10. Velocity profiles.

to guarantee a stable platoon pattern while vehicle 1 diverges from the platoon.

In terms of communication links, adjacency matrices in the order f $\rightarrow$ e $\rightarrow$ c in Table I follow Fig. 1-c left-middle-right, and describe the vehicle diverging maneuver. Vehicle 1 follows the procedures listed in Table VII.

In the experiments, vehicle 1 is used to perform a vehicle diverging maneuver as shown in Fig. 8. Then, a platoon with three equipped vehicles (vehicle 0, 2, and 3) moves on a lane, and vehicle 1 moves on an adjacent lane.

C. Results

This section discusses results of the field experiments.

In Fig. 9, the three maneuvers of platoon forming, vehicle merging, and vehicle diverging can be captured effectively. Specifically, vehicle 0 becomes the leader and broadcasts PSTMs. Vehicle 2 and 3 send PFRMs to the leader after receiving PSTMs. Finally, a platoon consisting of three vehicles(i.e., vehicle 0, 2 and 3) is formed at point A of Fig. 9 followed by the operations discussed in section IV-B-1. Hence, Fig. 9 shows that the trajectories of the three vehicles coincide at the point A. Also, at point A in Fig. 10, the velocities of vehicles are almost the same. It verifies that a three-vehicle platoon is formed. Note that the platoon including three vehicles continues to accelerate at point A to reach the desired velocity.

Vehicle 2 will decelerate to increases the longitudinal gap between vehicles 2 and 0. Consequently, vehicle 3 will also decelerate according to the state of vehicle 2. The deceleration operations of vehicles 2 and 3 can be captured before point B in Fig. 10. When the longitudinal gap between vehicles 2 and 0 is adequate, vehicle 1 will perform the merging

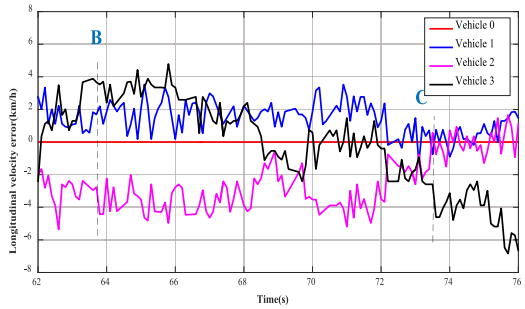

Fig. 11. Longitudinal velocity errors.

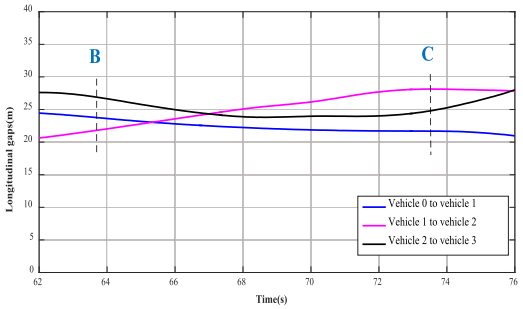

Fig. 13. Longitudinal gaps.

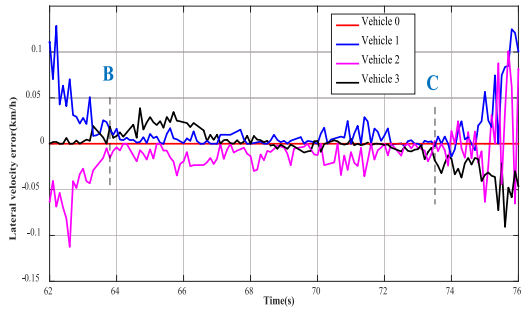

Fig. 12. Lateral velocity errors.

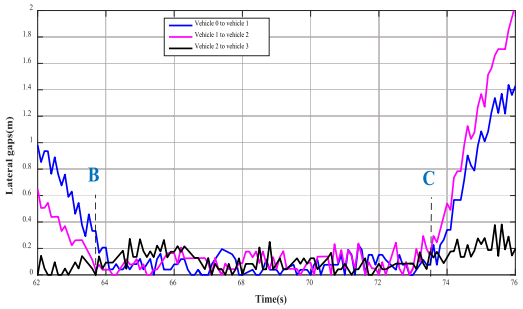

Fig. 14. Lateral gaps.

maneuver with a lane-change operation under the proposed algorithm (12).

During the experiments, parameters in (12) are set as [11]: $\delta = 1$, $\mu = 1$, $\rho = 1$, $r_{1,0} = 25$m, and $r_1 = 25$m. At point B in Fig. 9, vehicle 1 has merged into the platoon. Hence, the trajectories of the four vehicles coincide at point B in Fig. 9. In addition, the velocities of these vehicles are almost identical, and the platoon will move stably between points B and C in Fig. 10 with the velocity of 37 km/h. During this stage, the behavior of vehicles in the platoon can be described by the proposed car-following model (1) in section II. Here, parameters in (1) are set as [5]: $m = 0.41\text{s}^{-1}$, $\lambda = 0.1\text{s}^{-1}$, $\alpha_1 = 1$ and $p_1 = 1$. The velocity profile between point B and point C in Fig. 11 suggests that the follower vehicle can follow its predecessor effectively.

At 73s, vehicle 1 sends the VDRM to the leader in Fig. 10. After approval, vehicle 1 will perform the diverging maneuver using the lane-change operation and diverge from the platoon at point C in Fig. 9. Vehicles 0, 2 and 3 will keep the platoon pattern for a period. Then, each vehicle in the platoon will diverge one at a time and come to a stop, similar to vehicle 1. This can be observed after point C in Figs. 9 and 10.

Figs. 11 and 12 illustrate the longitudinal and lateral velocity errors, respectively. They are determined based on adjacent vehicle pairs. In Figs. 11 and 12, point B implies that vehicle 1 has merged into the platoon as the longitudinal velocity errors decrease and the lateral velocity errors approach 0km/h. At point C, vehicle 1 diverges from the platoon using a lane-change operation, resulting in large fluctuations in Figs. 11 and 12.

Figs. 13 and 14 show that the longitudinal and lateral gaps are maintained at about 25m and 0.2m, respectively, between point B and point C. It implies that the four-vehicle platoon is moving stably. In addition, the same stage in Figs. 11 and 12 shows that the four-vehicle platoon has small errors in velocity and inter-vehicle gap.

In summary, when the platoon moves stably, the longitudinal velocity errors will decrease and the lateral velocity errors will be maintained at 0km/h. While the longitudinal gaps are about 25m, the lateral gaps converge to a small range near 0m. In addition, the consensus of vehicles in the CV platoon can be guaranteed by the proposed control algorithm (15) and the car-following behavior between CVs in the platoon can be captured by the proposed car-following model (1) effectively.

V. Concluding Remarks

This study focuses on the platoon control of CVs under the V2X communications. For this purpose, the BDLF communication topology is developed to characterize the connections among CVs. Then, a consensus-based control algorithm is designed for platoon control. The consensus of the proposed control is analyzed using the Lyapunov technique. In addition, a new car-following model is proposed to describe the local interactions between CVs. The stability of the proposed car-following model is performed using the perturbation method. Finally, field experiments are conducted under the scenarios of platoon forming, vehicle merging, and vehicle diverging. Results from field experiments verify the effectiveness of the proposed method in terms of the trajectory, velocity, and inter-vehicle gap profiles.

The study findings provide insights for the emerging connected and automated transportation system future, specifically in terms of how vehicle platooning can be enabled to gain benefits for traffic congestion mitigation, road throughput

increase, and energy consumption. However, the control algorithm designed in this study is limited by the need to consider communication delays and communication packet drops, which is the focus of our ongoing work.

REFERENCES

[1] M. Torrent-Moreno, J. Mittag, P. Santi, and H. Hartenstein, "Vehicle-to-vehicle communication: Fair transmit power control for safety-critical information," *IEEE Trans. Veh. Technol.*, vol. 58, no. 7, pp. 3684–3703, Sep. 2009.

[2] X. Zhang, Y. Fang, J. Wang, and J. Yuan, "Multilevel human-like motion planning for mobile robots in complex indoor environments," *IEEE Trans. Autom. Sci. Eng.*, to be published. doi: 10.1109/TASE.2018.2880245.

[3] X. Zhang, R. Wang, Y. Fang, B. Li, and B. Ma, "Acceleration-level pseudo-dynamic visual servoing of mobile robots with backstepping and dynamic surface control," *IEEE Trans. Syst., Man, Cybern., Syst.*, to be published. doi: 10.1109/TSMC.2017.2777897.

[4] Y. Li, B. Yang, T. Zheng, Y. Li, M. Cui, and S. Peeta, "Extended-state-observer-based double-loop integral sliding-mode control of electronic throttle valve," *IEEE Trans. Intell. Transport. Syst.*, vol. 16, no. 5, pp. 2501–2510, Oct. 2015.

[5] Y. Li *et al.*, "Nonlane-discipline-based car-following model for electric vehicles in transportation-cyber-physical-systems," *IEEE Trans. Intell. Transport. Syst.*, vol. 19, no. 1, pp. 38–47, Jan. 2018.

[6] X. Cheng, C. Chen, W. Zhang, and Y. Yang, "5G-Enabled cooperative intelligent vehicular (5GenCIV) framework: When benz meets marconi," *IEEE Intell. Syst.*, vol. 32, no. 3, pp. 53–59, May/Jun. 2017.

[7] X. Cheng, L. Yang, and X. Shen, "D2D for intelligent transportation systems: A feasibility study" *IEEE Trans. Intell. Transport. Syst.*, vol. 16, no. 4, pp. 1784–1793, Aug. 2015.

[8] J. Ma, X. Li, F. Zhou, and W. Hao, "Designing optimal autonomous vehicle sharing and reservation systems: A linear programming approach," *Transp. Res. C, Emerg. Technol.*, vol. 84, pp. 124–141, Nov. 2017.

[9] C. Shao, S. Leng, Y. Zhang, A. Vinel, and M. Jonsson, "Performance analysis of connectivity probability and connectivity-aware MAC protocol design for platoon-based VANETs," *IEEE Trans. Veh. Technol.*, vol. 64, no. 12, pp. 5596–5609, Dec. 2015.

[10] D. Jia and D. Ngoduy, "Platoon based cooperative driving model with consideration of realistic inter-vehicle communication," *Transp. Res. C, Emerg. Technol.*, vol. 68, pp. 245–264, Jul. 2016.

[11] Y. Li, K. Li, T. Zheng, X. Hu, H. Feng, and Y. Li, "Evaluating the performance of vehicular platoon control under different network topologies of initial states," *Phys. A, Statist. Mech. Appl.*, vol. 450, pp. 359–368, May 2016.

[12] M. Kang and H.-S. Ahn, "Design and realization of distributed adaptive formation control law for multi-agent systems with moving leader," *IEEE Trans. Ind. Electron.*, vol. 63, no. 2, pp. 1268–1279, Feb. 2016.

[13] Y. Guo, C. Xiong, J. Ma, and X. Li, "Joint optimization of vehicle trajectories and intersection controllers with connected automated vehicles: Combined dynamic programming and shooting heuristic approach," *Transp. Res. C, Emerg. Technol.*, vol. 98, pp. 54–72, Jan. 2019.

[14] L. Xiao and F. Gao, "Practical string stability of platoon of adaptive cruise control vehicles," *IEEE Trans. Intell. Transp. Syst.*, vol. 12, no. 4, pp. 1184–1194, Dec. 2011.

[15] Y. Li, C.Tang, S. Peeta, and Y. Wang, "Integral-sliding-mode braking control for a connected vehicle platoon: Theory and application," *IEEE Trans. Ind. Electron.*, vol. 66, no. 6, pp. 4618–4628, Jun. 2019.

[16] Y. Li, C.Tang, S. Peeta, and Y. Wang, "Nonlinear consensus-based connected vehicle platoon control incorporating car-following interactions and heterogeneous time delays," *IEEE Trans. Intell. Transport. Syst.*, to be published. doi: 10.1109/TITS.2018.2865546.

[17] A. Ghasemi, R. Kazemi, and S. Azadi, "Stable decentralized control of a platoon of vehicles with heterogeneous information feedback," *IEEE Trans. Veh. Technol.*, vol. 62, no. 9, pp. 4299–4308, Nov. 2013.

[18] X. Guo, J. Wang, F. Liao, and R. S. H. Teo, "Distributed adaptive integrated-sliding-mode controller synthesis for string stability of vehicle platoons," *IEEE Trans. Intell. Transp. Syst.*, vol. 17, no. 9, pp. 2419–2429, Apr. 2016.

[19] W. B. Dunbar and D. S. Caveney, "Distributed receding horizon control of vehicle platoons: Stability and string stability," *IEEE Trans. Autom. Control*, vol. 56, no. 3, pp. 620–633, Mar. 2012.

[20] M. D. Bernardo, A. Salvi, and S. Santini, "Distributed consensus strategy for platooning of vehicles in the presence of time-varying heterogeneous communication delays," *IEEE Trans. Intell. Transp. Syst.*, vol. 16, no. 1, pp. 102–112, Feb. 2015.

[21] S. E. Li, F. Gao, D. Cao, and K. Li, "Multiple-model switching control of vehicle longitudinal dynamics for platoon-level automation," *IEEE Trans. Veh. Technol.*, vol. 65, no. 6, pp. 4480–4492, Jun. 2016.

[22] X. Yu and L. Liu, "Distributed formation control of nonholonomic vehicles subject to velocity constraints," *IEEE Trans. Ind. Electron.*, vol. 63, no. 2, pp. 1289–1298, Feb. 2016.

[23] M. Defoort, T. Floquet, A. Kokosy, and W. Perruquetti, "Sliding-mode formation control for cooperative autonomous mobile robots," *IEEE Trans. Ind. Electron.*, vol. 55, no. 11, pp. 3944–3953, Nov. 2008.

[24] H. Su, M. Z. Q. Chen, X. Wang, and J. Lam, "Semiglobal observer-based leader-following consensus with input saturation," *IEEE Trans. Ind. Electron.*, vol. 61, no. 6, pp. 2842–2850, Jun. 2014.

[25] J. Qin, C. Yu, and H. Gao, "Coordination for linear multiagent systems with dynamic interaction topology in the leader-following framework," *IEEE Trans. Ind. Electron.*, vol. 61, no. 5, pp. 2412–2422, May 2014.

[26] K. You and L. Xie, "Network topology and communication data rate for consensusability of discrete-time multi-agent systems," *IEEE Trans. Autom. Control*, vol. 56, no. 10, pp. 2262–2275, Oct. 2011.

[27] H. Zhang, H. Jiang, Y. Luo, and G. Xiao, "Data-Driven optimal consensus control for discrete-time multi-agent systems with unknown dynamics using reinforcement learning method," *IEEE Trans. Ind. Electron.*, vol. 64, no. 5, pp. 4091–4100, May 2017.

[28] H. Zhang, G. Feng, H. Yan, and Q. Chen, "Observer-based output feedback event-triggered control for consensus of multi-agent systems," *IEEE Trans. Ind. Electron.*, vol. 61, no. 9, pp. 4885–4894, Sep. 2014.

[29] Y. Li, C. Tang, K. Li, S. Peeta, X. He, and Y. Wang, "Nonlinear finite-time consensus-based connected vehicle platoon control under fixed and switching communication topologies," *Transp. Res. C, Emerg. Technol.*, vol. 93, pp. 525–543, Aug. 2018.

[30] Y. Li, C. Tang, K. Li, X. He, S. Peeta, and Y. Wang, "Consensus-based cooperative control for multi-platoon under the connected vehicles environment," *IEEE Trans. Intell. Transport. Syst.*, to be published. doi: 10.1109/TITS.2018.2865575.

[31] P. Seiler, A. Pant, and K. Hedrick, "Disturbance propagation in vehicle strings," *IEEE Trans. Autom. Control*, vol. 49, no. 10, pp. 1835–1842, Oct. 2004.

[32] Y. Zheng, S. E. Li, K. Li, and L.-Y. Wang, "Stability margin improvement of vehicular platoon considering undirected topology and asymmetric control," *IEEE Trans. Control Syst. Technol.*, vol. 24, no. 4, pp. 1253–1265, Jul. 2016.

[33] D. Jia and D. Ngoduy, "Enhanced cooperative car-following traffic model with the combination of V2V and V2I communication," *Transport. Res. B, Methodol.*, vol. 90, pp. 172–191, Aug. 2016.

[34] Y. Zheng, S. Eben Li, J. Wang, D. Cao, and K. Li, "Stability and scalability of homogeneous vehicular platoon: Study on the influence of information flow topologies," *IEEE Trans. Intell. Transport. Syst.*, vol. 17, no. 1, pp. 14–26, Jan. 2016.

[35] C. Campolo, A. Vinel, A. Molinaro, and Y. Koucheryavy, "Modeling broadcasting in IEEE 802.11p/WAVE vehicular networks," *IEEE Commun. Lett.*, vol. 15, no. 2, pp. 199–201, Feb. 2011.

[36] W. Alasmary and W. Zhuang, "Mobility impact in IEEE 802.11p infrastructureless vehicular networks," *Ad Hoc Netw.*, vol. 10, no. 2, pp. 222–230, Mar. 2012.

[37] M. Bando, K. Hasebe, A. Nakayama, A. Shibata, and Y. Sugiyama, "Dynamics model of traffic congestion and numerical simulation," *Phys. Rev. E, Stat. Phys. Plasmas Fluids Relat. Interdiscip. Top.*, vol. 51, no. 2, pp. 1035–1042, Feb. 1995.

[38] R. Jiang, Q. Wu, and Z. Zhu, "Full velocity difference model for a car-following theory," *Phys. Rev. E, Stat. Phys. Plasmas Fluids Relat. Interdiscip. Top.*, vol. 64, no. 1, pp. 017101–017105, Jun. 2001.

[39] Y. Liu and B. Xu, "Improved protocols and stability analysis for multivehicle cooperative autonomous systems," *IEEE Trans. Intell. Transp. Syst.*, vol. 16, no. 5, pp. 2700–2710, Oct. 2015.

[40] P. Parks and V. Hahn, *Stability Theory*. Englewood Cliffs, NJ, USA: Prentice-Hall, 1992.

[41] J. Kown and D. Chwa, "Adaptive bidirectional platoon control using a coupled sliding mode control method," *IEEE Trans. Intell. Transport. Syst.*, vol. 15, no. 5, pp. 2040–2048, Oct. 2014.

[42] Z. Zhao, M. Wen, C.-X. Wang, X. Cheng, and B. Jiao, "Channel estimation schemes for IEEE 802.11p standard," *IEEE Intel. Transport. Syst. Mag.*, vol. 5, no. 4, pp. 38–49, Dec. 2013.

Yongfu Li (M'16) received the Ph.D. degree in control science and engineering from Chongqing University, Chongqing, China, in 2012.

He is currently a Full Professor of control science and engineering with the Chongqing University of Posts and Telecommunications and the Director of the Key Laboratory of Intelligent Air-Ground Cooperative Control for Universities in Chongqing. His research interests include connected and automated vehicles, intelligent transportation systems, and cooperative control theory and application.

Dr. Li has served as a member of the Technical Committee on Vehicle Control and Intelligence of the Chinese Association of Automation (CAA).

Wenbo Chen received the B.S. degree in communication engineering from the Chongqing University of Posts and Telecommunications, Chongqing, China, in 2016, where he is currently pursuing the M.S. degree in control science and engineering.

His research interests include platoon control, intelligent transportation systems, and connected vehicles.

Srinivas Peeta received the Ph.D. degree in civil engineering from The University of Texas at Austin, Austin, TX, USA, in 1994.

He is currently the Frederick R. Dickerson Chair and a Professor with the School of Civil and Environmental Engineering and the School of Industrial and Systems Engineering, Georgia Institute of Technology. He is also a Principal Research Faculty with the Georgia Tech Research Institute. His research interests include intelligent transportation systems and connected and automated vehicles.

Yibing Wang (M'03) received the Ph.D. degree in control theory and applications from Tsinghua University, Beijing, China.

He is currently a Full Professor with the College of Civil Engineering and Architecture, Institute of Transportation Engineering, Zhejiang University, Hangzhou, China. His research interests include traffic flow modeling, freeway traffic surveillance, ramp metering, urban traffic signal control, and vehicular ad hoc networks.